Chapter 22
RBFNN-Based Path Following Adaptive Control for Underactuated Surface Vessels

Wei Meng and Chen Guo

Abstract A robust adaptive control strategy is developed to force an underactuated surface vessel to follow a reference path at a desired speed with the unknown parameters, despite the presence of environmental disturbances induced by wave, wind, and ocean current. The proposed controller is designed by using RBF neural networks and the backstepping techniques. The proposed control system allows for both low- and high-speed applications since linear and nonlinear damping terms were considered in the control design. Numerical simulation results are provided to demonstrate the effectiveness of the proposed controller design and the accuracy of stability analysis.

Keywords Underactuated surface vessels · Path following · RBF neural networks · Adaptive control

22.1 Introduction

Robust path following is an issue of vital practical importance to the ship industry. For the path following problem, the main challenge is that most ships are usually equipped with one or two main propellers for surge motion control, and rudders for yaw motion control of the ship. There are no side thrusters, so the sway axis is not actuated. This configuration is mostly used in the marine vehicles [1]. Meanwhile, another challenge of path following issue is the inherent nonlinearity of the ship dynamics and kinematics with the uncertain parameters and unstructured

W. Meng (✉)
School of Information Engineering, Dalian Ocean University, Dalian 116023, China
e-mail: mengwei6699@126.com

C. Guo
School of Information Science and Technology, Dalian Maritime University,
Dalian 116026, China
e-mail: guoc@dlmu.edu.cn

Z. Deng and H. Li (eds.), *Proceedings of the 2015 Chinese Intelligent Automation Conference*, Lecture Notes in Electrical Engineering 337,
DOI 10.1007/978-3-662-46463-2_22

uncertainties including external disturbances and measurement noise, etc. To overcome these challenges, many different nonlinear design methodologies have been introduced to the underactuated ships. By applying the Lyapunov's direct method, two constructive tracking solutions were developed in Jiang [2]. In [3–5], the controllers were designed to force an underactuated surface vessel to follow a predefined path. The stability analysis was investigated relying on the Lyapunov's direct method. A robust adaptive control scheme was proposed for point-to-point navigation of underactuated ships by using a general backstepping technique [6]. In [7], a simple control law was presented by using the novel backstepping and feedback dominance. Furthermore, the control design was verified using a model ship in a tank. By using intelligent control, Liu proposed a stable adaptive neural network algorithm for the path following of underactuated ship with parameters uncertainties and disturbances [8].

Motivated by these recent developments in path following of underactuated surface vessels, this paper presents an adaptive RBF neural networks control law. The stability analysis is performed based on the Lyapunov theory. The proposed controller can guarantee that all signals of the underactuated system are bounded. Numerical simulations are provided to validate the effectiveness of the proposed path following controller.

22.2 Problem Statements

Consider the path following problem of an underactuated surface vessel. Generally, for path following, the vessel is moving in the horizontal plane, the heave, roll, and pitch are normally neglected. The mathematical model of the underactuated surface vessel moving in three degrees of freedom can be described as [9]:

$$\begin{cases} \dot{x} = u\cos\psi - v\sin\psi \\ \dot{y} = u\sin\psi + v\cos\psi \\ \dot{\psi} = r \\ \dot{u} = f_u(u,v,r) + \tau_u/m_{11} + b_u/m_{11} \\ \dot{v} = f_v(u,v,r) + b_v/m_{22} \\ \dot{r} = f_r(u,v,r) + \tau_r/m_{33} + b_r/m_{33} \end{cases} \tag{22.1}$$

with $f_u = m_{22}vr/m_{11} - d_u u/m_{11} - \sum_{i=2}^{3} d_{ui}|u|^{i-1}u/m_{11}$, $f_v = -m_{11}ur/m_{22} - d_v v/m_{22} - \sum_{i=2}^{3} d_{vi}|v|^{i-1}v/m_{22}$, $f_r = (m_{11}-m_{22})uv/m_{33} - d_r r/m_{33} - \sum_{i=2}^{3} d_{ri}\,|r|^{i-1}r/m_{33}$, $[b_u, b_v, b_r]^T = R(\psi)^T\left[b_x, b_y, b_\psi\right]^T$, $R(\psi) = \begin{bmatrix} \cos\psi & -\sin\psi & 0 \\ \sin\psi & \cos\psi & 0 \\ 0 & 0 & 1 \end{bmatrix}$.

where x, y, and ψ are the surge displacement, sway displacement, and the yaw angle in the earth fixed frame, and u, v, and r are the velocities in surge, sway, and yaw, respectively. The constant parameters $m_{jj} > 0$, $1 \le j \le 3$, denote the ship's inertia and added mass effects. The positive terms $d_u, d_v, d_r, d_{ui}, d_{vi}$, and d_{ri}, $i = 2, 3$, are given by the hydrodynamic damping in surge, sway, and yaw. τ_u and τ_r denote the available control inputs, respectively, the surge force and the yaw moment. $b = \left[b_x, b_y, b_\psi\right]^T$ denote the low frequency interference in the earth fixed frame, $\dot{b} = 0$.

We now define the path following errors in a frame attached to the path as follows [8]:

$$(x_e, y_e, \psi_e)^T = R^T(\psi)(x - x_d, y - y_d, \psi - \psi_d)^T, \tag{22.2}$$

where ψ_d represents the desired yaw angle and was defined as $\psi_d = \arctan\left(y'_d(s)/x'_d(s)\right)$, $x'_d = \partial x_d/\partial s$, $y'_d = \partial y_d/\partial s$; x_d and y_d denote the desired displacement in path of the vessel.

Assumption 22.1 The parameters of underactuated surface vessels such as m_{jj}, d_u, d_v, d_r, d_{ui}, d_{vi}, and d_{ri}, $1 \le j \le 3$, $i = 2, 3$, are known.

Assumption 22.2 The reference path is regular, x_d, $\dot{x}_d$, $\ddot{x}_d$, y_d, $\dot{y}_d$, $\ddot{y}_d$, $\dot{\psi}_d$ and $\ddot{\psi}_d$ are all bounded.

Control objective: Under Assumptions 22.1 and 22.2, the objective of this paper is to seek the adaptive control laws τ_u and τ_r that force the vessel from the initial position and orientation to follow a reference path $\mathbf{\Omega}$.

22.3 Control Design

In this section, we develop an adaptive control law for underactuated surface vessels (22.1) with uncertain dynamics.

From (22.2), we have

$$\begin{cases} \dot{x}_e = u - u_d\cos(\psi_e) + ry_e \\ \dot{y}_e = v + u_d\sin(\psi_e) - rx_e \\ \dot{\psi}_e = r - rd \end{cases} \tag{22.3}$$

where $u_d = \bar{u}_d\dot{s}$, $\bar{u}_d = \sqrt{x'^2_d(s) + y'^2_d(s)}$, $r_d = \frac{x'^2_d(s)y''^2_d(s) - x''^2_d(s)y'^2_d(s)}{x'^2_d(s) + y'^2_d(s)}\dot{s}$.

We define

$$u_e = u - \alpha_u, \bar{\psi}_e = \psi_e - \alpha_{\psi_e} \tag{22.4}$$

where α_u and α_{ψ_e} are virtual controls of u and ψ_e. Substituting (22.4) into (22.3) results in

$$\begin{cases} \dot{x}_e = \alpha_u + u_e - u_d\cos(\psi_e) + \Delta_1 + ry_e \\ \dot{y}_e = v + u_d\sin(\psi_e) + \Delta_2 - rx_e \end{cases} \tag{22.5}$$

where $\Delta_1 = -u_d\left(\left(\cos\left(\bar{\psi}_e\right) - 1\right)\cos\left(\alpha_{\psi_e}\right) - \sin\left(\bar{\psi}_e\right) \quad \sin\left(\alpha_{\psi_e}\right)\right), \Delta_2 = u_d\sin\left(\bar{\psi}_e\right)$ $\cos\left(\alpha_{\psi_e}\right) + \left(\cos\left(\bar{\psi}_e\right) - 1\right)\sin\left(\alpha_{\psi_e}\right)$.

We choose the virtual control α_u as

$$\alpha_u = -k_1x_e + u_d\cos\left(\alpha_{\psi_e}\right) \tag{22.6}$$

where $k_1 > 0$. The derivative of the path parameter s satisfies

$$\dot{s} = \sqrt{u_{d0}^2 + (k_2y_e + v_d)^2}\Big/\bar{u}_d \tag{22.7}$$

where $k_2 > 0$, v_d is the filter of v, $v_e = v - v_d$. From (22.7), we have

$$u_d = \sqrt{u_{d0}^2 + (k_2y_e + v_d)^2} \tag{22.8}$$

We choose the virtual control α_{ψ_e} as

$$\alpha_{\psi_e} = -\arctan((k_2y_e + v_d)/u_{d0}) \tag{22.9}$$

Substituting (22.6), (22.7), and (22.9) into (22.5), we have

$$\begin{cases} \dot{x}_e = -k_1x_e + u_e + \Delta_1 + ry_e \\ \dot{y}_e = -k_2y_e + v_e + \Delta_2 - rx_e \end{cases} \tag{22.10}$$

And substituting (22.9) into (22.6), we have

$$\alpha_u = -k_1x_e + u_{d0} \tag{22.11}$$

The time derivative of (22.4) using (22.3) and (22.9) can be derived as

$$\dot{\bar{\psi}}_e = r - r_d + \{[k_2(-k_2y_e - rx_e + \Delta_2 + v_e) + \dot{v}_d]u_{d0} - (k_2y_e + v_d)\dot{u}_{d0}\}\big/u_d^2 \tag{22.12}$$

We define the r_e as

$$r_e = r - \alpha_r \tag{22.13}$$

Substituting (22.13) into (22.12), we have

$$\dot{\bar{\psi}}_e = -k_3\bar{\psi}_e + f_x r_e + k_2 u_{d0} v_e / u_d^2 \tag{22.14}$$

where $k_3 > 0$, $f_x = 1 - k_2 x_e u_{d0} / u_d^2$.

Differentiating v_e, and substituting (22.1) into it, we have

$$v_e = g_v - \dot{v}_d \tag{22.15}$$

where $g_v = f_v(u, v, r) + b_v / m_{22}$.

According to the approximation property of NNs, the smooth function g_v can be approximated by RBF neural networks as follows

$$g_v = W_v^T \sigma(\eta) + \varepsilon_v \tag{22.16}$$

where W_v is the idea weight matrix, ε_v is the approximation error, $|\varepsilon_v| \le \varepsilon_{vM}$, $\eta = [x, y, \psi, u, v, r]^T$.

Let $\hat{W}_v$ be the estimations of the weights W_v, $\hat{g}_v$ is the estimation of the g_v, and can be defined as

$$\hat{g}_v = \hat{W}_v^T \sigma(\eta) \tag{22.17}$$

In order to stabilize the v_e, the $\dot{v}_d$ can be chosen as

$$\dot{v}_e = \hat{W}_v^T \sigma(\eta) - k_6 v_e - k_2 u_{d0} \bar{\psi}_e / u_d^2 + \varepsilon_v \tag{22.18}$$

The time derivative of (22.4) can be derived

$$\dot{u}_e = g_u + \tau_u / m_{11} - \dot{\alpha}_u \tag{22.19}$$

with $g_u = f_u(u, v, r) + b_u / m_{11}$, $\dot{\alpha}_u = \dfrac{\partial \alpha_u}{\partial x_e}\dot{x}_e + \dfrac{\partial \alpha_u}{\partial u_{d0}}\dot{u}_{d0}$.

The smooth function g_u can also be approximated by RBF neural networks as follows

$$g_u = W_u^T \sigma(\eta) + \varepsilon_u \tag{22.20}$$

where W_u is the idea weight matrix, ε_u is the approximation error, $|\varepsilon_v| \le \varepsilon_{vM}$, $\eta = [x, y, \psi, u, v, r]^T$.

Let $\hat{W}_u$ be the estimations of the weights W_u, $\hat{g}_u$ is the estimation of the g_u, and can be defined as

$$\hat{g}_u = \hat{W}_u^T \sigma(\eta) \tag{22.21}$$

The time derivative of (22.13) can be derived as

$$\dot{r}_e = g_r + \tau_r/m_{33} - \dot{\alpha}_r \tag{22.22}$$

where $g_r = f_r(u, v, r) + b_r/m_{33} + \dot{\hat{g}}_v$.

The smooth function g_u can be approximated by RBF neural networks as follows

$$g_r = W_r^T \sigma(\eta) + \varepsilon_r \tag{22.23}$$

where W_r is the idea weight matrix, ε_r is the approximation error, $|\varepsilon_r| \leq \varepsilon_{rM}$, $\eta = [x, y, \psi, u, v, r]^T$.

Let $\hat{W}_r$ be the estimations of the weights W_r, $\hat{g}_r$ is the estimation of the g_r, and can be defined as

$$\hat{g}_r = \hat{W}_r^T \sigma(\eta) \tag{22.24}$$

From (22.19) and (22.22), the adaptive NNs surge control law τ_u and the yaw moment control law τ_r can be presented as

$$\tau_u = m_{11}(-\hat{g}_u - k_4 u_e + \dot{\alpha}_u), \quad k_4 > 0 \tag{22.25}$$

$$\tau_r = m_{33}\left(-\hat{g}_r - k_5 r_e + \dot{\alpha}_r - f_x \bar{\psi}_e\right), \quad k_5 > 0 \tag{22.26}$$

The adaptive laws are given by

$$\dot{\hat{W}}_u = \Gamma_u\left[\sigma(\eta) u_e - k_u \hat{W}_u\right] \tag{22.27}$$

$$\dot{\hat{W}}_v = \Gamma_v\left[\sigma(\eta) v_e - k_v \hat{W}_v\right] \tag{22.28}$$

$$\dot{\hat{W}}_r = \Gamma_r\left[\sigma(\eta) r_e - k_r \hat{W}_r\right] \tag{22.29}$$

where $\Gamma_u = \Gamma_u^T > 0$, $\Gamma_v = \Gamma_v^T > 0$, $\Gamma_r = \Gamma_r^T > 0$ are constant design parameters.

22.4 Stability Analysis

Theorem 22.1 Assume that the Assumptions 1–2 hold, the adaptive NNs surge control law τ_u and the yaw moment control law τ_r are derived as in (22.25) and (22.26), and adaptation laws are given by (22.27–22.29), the control objective of path following for underactuated surface vessels in the presence of uncertain parameters and unstructured uncertainties is solved, and the systems (22.1) are asymptotic stability.

Proof From (22.29) and (22.30), we have

$$\begin{cases} \dot{Z}_1 = f_1(Z_1, Z_2) \\ \dot{Z}_2 = f_2(Z_2) \end{cases}, \tag{22.30}$$

with $Z_1 = [x_e, y_e]^T$, $Z_2 = \left[\bar{\psi}_e, u_e, v_e, r_e, \tilde{W}_u, \tilde{W}_v, \tilde{W}_r\right]^T$

$$\begin{aligned} f_1 &= [-k_1 x_e + u_e + \Delta_1 + r y_e, -k_2 y_e + v_e + \Delta_2 - r x_e]^T, \\ f_2 &= \left[-k_3 \bar{\psi}_e + f_x r_e + k_2 u_{d0} v_e / u_d^2, \tilde{W}_u^T \sigma(\eta) - k_4 u_e + \varepsilon_u, \tilde{W}_v^T \sigma(\eta)\right. \\ &\quad - k_6 v_e - k_2 u_{d0} \bar{\psi}_e / u_d^2 + \varepsilon_v, \tilde{W}_r^T \sigma(\eta) - k_5 r_e - f_x \bar{\psi}_e + \varepsilon_r, \\ &\quad \left. -\Gamma_u\left[\sigma(\eta) u_e - \sigma_u \hat{W}_u\right], -\Gamma_v\left[\sigma(\eta) v_e - \sigma_v \hat{W}_v\right], -\Gamma_r\left[\sigma(\eta) r_e - \sigma_r \hat{W}_r\right]\right]^T. \end{aligned}$$

To investigate stability of this subsystem, we consider the following Lyapunov function:

$$V_1 = \frac{1}{2}\bar{\psi}_e^2 + \frac{1}{2}u_e^2 + \frac{1}{2}r_e^2 + \frac{1}{2}\tilde{W}_u^T \Gamma_u^{-1} \tilde{W}_u + \frac{1}{2}\tilde{W}_v^T \Gamma_v^{-1} \tilde{W}_v + \frac{1}{2}\tilde{W}_r^T \Gamma_r^{-1} \tilde{W}_r, \tag{22.31}$$

Differentiating (22.32) along with (22.27–22.30), we have

$$\begin{aligned} \dot{V}_1 \leq & -k_3 \bar{\psi}_e^2 - k_4 u_e^2 - k_5 r_e^2 - k_6 v_e^2 + \sigma_u \tilde{W}_u^T \hat{W}_u + \sigma_v \tilde{W}_v^T \hat{W}_v + \sigma_r \tilde{W}_r^T \hat{W}_r \\ & + u_e \varepsilon_u + v_e \varepsilon_v + r_e \varepsilon_r \end{aligned} \tag{22.32}$$

The (22.33) can be described as

$$\begin{aligned} \dot{V}_1 \leq & -k_3 \bar{\psi}_e^2 - \left(k_4 - \frac{1}{4}\right) u_e^2 - \left(k_5 - \frac{1}{4}\right) v_e^2 - \left(k_6 - \frac{1}{4}\right) r_e^2 \\ & -\frac{1}{2}\sigma_u \left\|\tilde{W}_u\right\|^2 - \frac{1}{2}\sigma_v \left\|\tilde{W}_v\right\|^2 \\ & -\frac{1}{2}\sigma_r \left\|\tilde{W}_r\right\|^2 + \varepsilon_u^2 + \varepsilon_v^2 + \varepsilon_r^2 + \frac{1}{2}\sigma_u \|W_u\|^2 + \frac{1}{2}\sigma_v \|W_v\|^2 + \frac{1}{2}\sigma_r \|W_r\|^2 \\ \leq & -\mu V_1 + \rho \end{aligned} \tag{22.33}$$

with
$\mu := \min\left\{2k_3, 2\left(k_4 - \frac{1}{4}\right), 2\left(k_5 - \frac{1}{4}\right), 2\left(k_6 - \frac{1}{4}\right), \min\left(\frac{\sigma_u}{\lambda_{\max}(\Gamma_u^{-1})}\right), \min\left(\frac{\sigma_v}{\lambda_{\max}(\Gamma_v^{-1})}\right),\right.$
$\left.\min\left(\frac{\sigma_r}{\lambda_{\max}(\Gamma_r^{-1})}\right)\right\}$, $\rho := \varepsilon_u^2 + \varepsilon_v^2 + \varepsilon_r^2 + \frac{\sigma_u}{2}\|W_u\|^2 + \frac{\sigma_v}{2}\|W_v\|^2 + \frac{\sigma_r}{2}\|W_r\|^2$

Let $\Phi = \frac{\varrho}{\mu}$, the (22.34) can be rewritten as

$$0 \leq V(t) \leq \Phi + [V(0) - \Phi]e^{-\mu t} \tag{22.34}$$

Hence, all signals of the closed-loop system are uniformly ultimately bounded. The path following errors will converge to a small neighborhood of zero, and can be adjusted by the design parameters $k_3, k_4, k_5, k_6, \sigma_u, \sigma_v, \sigma_r$.

22.5 Numerical Simulations

In this section, some numerical simulations are provided to demonstrate the effectiveness of the proposed control laws and the accuracy of stability analysis. In this paper, we use a monohull ship with the length of 38 m, mass of 118×10^3 kg, the numerical values of the vessel are adapted from [6].

In the simulation, the reference path is generated by a virtual ship as follows:

$$\begin{cases} \dot{x}_d = u_d \cos(\psi_d) - v_d \sin(\psi_d) \\ \dot{y}_d = u_d \sin(\psi_d) + v_d \cos(\psi_d) \\ \dot{\psi}_d = r_d \\ \dot{v}_d = -\dfrac{m_{11}}{m_{22}} u_d r_d - \dfrac{d_{22}}{m_{22}} v_d - \sum\limits_{i=2}^{3} \dfrac{d_{vi}}{m_{22}} |v_d|^{i-1} v_d \end{cases}$$

In the simulation we select $u_d = 5$, $r_d = 0.015$; the control parameters selected for the simulation are: $k_1 = 15$, $k_2 = 7.5$, $k_3 = 12$, $k_4 = 10$, $k_5 = 10$, $k_6 = 10$, $\Gamma_u = 10$, $\Gamma_v = 30$, $\Gamma_r = 0.5$, $\sigma_u = \sigma_v = \sigma_r = 0.01$,

The initial conditions are chosen as:

$$[x(0), y(0), \psi(0), u(0), v(0), r(0)] = [-100, 0, 0, 0, 0, 0].$$

The simulation results of ship path following control are plotted in Figs. 22.1 and 22.2. Figure 22.1 shows the position and the orientation of the vessel in the xy plane, and the control inputs τ_u and τ_r are plotted. The path following position errors are plotted in Fig. 22.2. It can be seen from these figures that all the signals of the closed-loop system are bounded. From Fig. 22.2, the path following position errors x_e, y_e, the velocity errors u_e, r_e, and the orientation error ψ_e converge to zero while the sway motion error v_e converges to a small value, since the reference path is generated by a virtual ship, the sway velocity error is always a constant value.

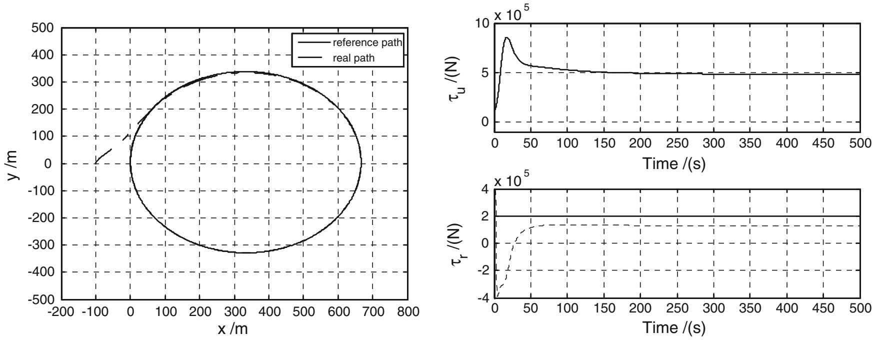

Fig. 22.1 Position and orientation and the inputs of the vessel

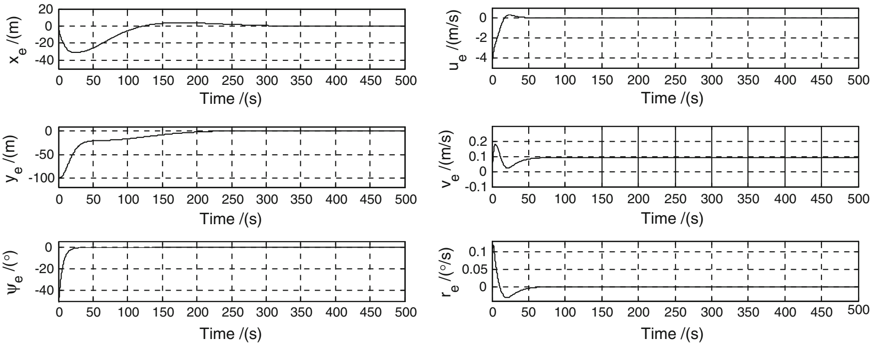

Fig. 22.2 Position, orientation, and velocity errors of the vessel

22.6 Conclusions

In this paper, we present an adaptive RBF neural networks scheme for path following of underactuated surface vessels with uncertain parameters and unstructured uncertainties including exogenous disturbances and measurement noise, etc. The proposed controller is designed by using RBF neural networks and the backstepping techniques. It is noted that the proposed control system allows for both low- and high-speed applications since linear and nonlinear damping terms were considered in the control design. The stability analysis is performed based on the Lyapunov theory. The effectiveness of the designed controller is also validated by the numerical simulations. Based on the ideas of this paper, the future work will consider the rudder saturation and rate limits.

Acknowledgments The work for this paper was financially supported by the National Natural Science Foundation of China (NSFC, Grant No: 61374114) and the Fundamental Research Funds for the Central Universities (Grant No: 3132014321).

References

1. Fossen TI (2002) Marine control systems. Marine Cybernetics, Trondheim
2. Jiang ZP (2002) Global tracking control of underactuated ships by Lyapunove's direct method. Automatica 38:301–309
3. Do KD, Jiang ZP, Pan J (2004) Robust adaptive path following of underactuated ships. Automatica 40:929–944
4. Do KD, Pan J (2004) State-and output-feedback robust path-following controllers for underactuated ships using Serret-Frenet frame. Ocean Eng 31:587–613
5. Do KD, Pan J (2006) Global robust adaptive path following of underactuated ships. Automatica 42:1713–1722
6. Li JH, Lee PM, Jun BH, Lim YK (2008) Point-to-point navigation of underactuated ships. Automatica 44:3201–3205
7. Li Z, Sun J, Oh SR (2009) Design, analysis and experimental validation of robust nonlinear path following control of marine surface vessels. Automatica 45:1649–1658
8. Liu Y, Guo C (2014) Control method of underactuated surface ship formation based on stable adaptive neural network control law. J Traffic Transp Eng 14(3):120–126
9. Perez T (2005) Ship motion control: course keeping and roll stabilisation using rudder and fins. Springer, Berlin